

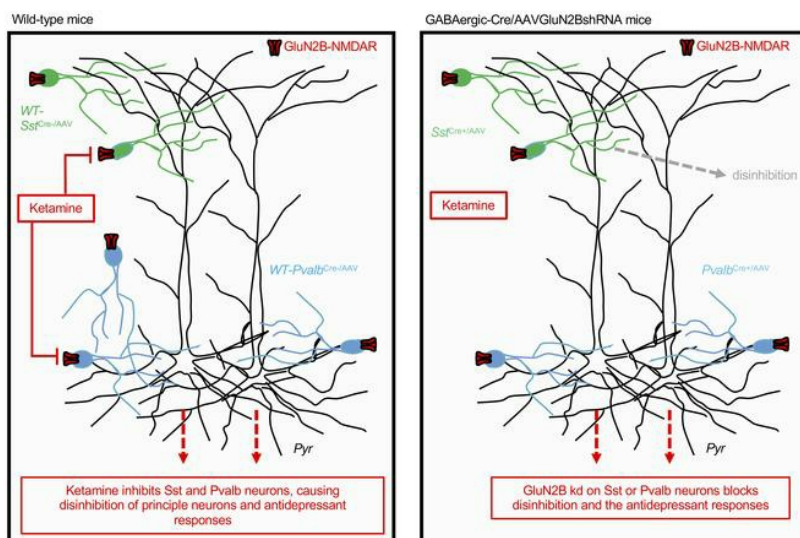
GABA interneurons are the cellular trigger for ketamine's rapid antidepressant actions

Danielle M. Gerhard, ... , Eric S. Wohleb, Ronald S. Duman

J Clin Invest. 2019. <https://doi.org/10.1172/JCI130808>.

Research In-Press Preview Neuroscience

Graphical abstract



Find the latest version:

<https://jci.me/130808/pdf>



GABA interneurons are the cellular trigger for ketamine's rapid antidepressant actions

Danielle M. Gerhard^{1,2,†}, Santosh Pothula^{2,†}, Rong-Jian Liu², Min Wu², Xiao-Yuan Li², Matthew J. Girgenti², Seth R. Taylor^{2,3}, Catharine H. Duman², Eric Delpire⁴, Marina Picciotto², Eric S. Wohleb^{2,5}, Ronald S. Duman^{*2}

¹Department of Psychiatry, Weill Cornell Medicine, New York, NY 10065, USA

²Department of Psychiatry, Yale School of Medicine, New Haven, CT 06511, USA

³Department of Cell and Developmental Biology, Vanderbilt University, Nashville, TN 37235,
USA

⁴Department of Anesthesiology, Vanderbilt University Medical School, Nashville, TN 37232,
USA

⁵Department of Pharmacology & Systems Physiology, University of Cincinnati College of
Medicine, Cincinnati, OH, 45237, USA

*Correspondence: Ronald Duman; address: Psychiatry, 34 Park Street, New Haven, CT, 06509, USA; telephone: 203-974-7726; email: ronald.duman@yale.edu.

†These authors contributed equally to this work

Conflict-of-interest statement: The authors have declared that no conflict of interest exists.

Abstract

A single sub-anesthetic dose of ketamine, an NMDA receptor (NMDAR) antagonist, produces rapid and sustained antidepressant actions in depressed patients, addressing a major unmet need for the treatment of mood disorders. Ketamine produces a rapid increase in extracellular glutamate and synaptic formation in the prefrontal cortex, but the initial cellular trigger that initiates these and its behavioral actions has not been identified. To address this question, we used a combination of viral shRNA and conditional mutation to produce cell specific knockdown or deletion of a key NMDAR subunit, GluN2B, implicated in the actions of ketamine. The results demonstrate that the antidepressant actions of ketamine were blocked by GluN2B-NMDAR knockdown on GABA (*Gad1*) interneurons, as well as subtypes expressing somatostatin (*Sst*), or parvalbumin (*Pvalb*), but not glutamate principle neurons in the mPFC. Further analysis of GABA subtypes showed that cell specific knockdown or deletion of GluN2B in *Sst* interneurons blocked or occluded the antidepressant actions of ketamine and revealed sex-specific differences that are associated with excitatory postsynaptic currents on mPFC principle neurons. These findings demonstrate that GluN2B-NMDARs on GABA interneurons are the initial cellular trigger for the rapid antidepressant actions of ketamine and show sex-specific adaptive mechanisms to GluN2B modulation.

Introduction

The N-methyl-D-aspartate receptor (NMDAR) antagonist ketamine produces rapid-acting antidepressant effects in both clinical studies of depressed patients and preclinical rodent models (1, 2). Although traditionally used as an anesthetic, over a decade of research has been devoted to unraveling the mechanisms responsible for the rapid antidepressant effects of ketamine. These efforts have uncovered a complex signaling cascade that results in activity-dependent synapse formation and reversal of the synaptic deficits caused by chronic stress exposure (2-4). Early studies using a sub-anesthetic dose of ketamine found a rapid and transient increase in glutamate release in the medial prefrontal cortex (mPFC) (5). This glutamate burst is believed to initiate activity-dependent release of brain-derived neurotrophic factor and stimulation of protein synthesis dependent synapse formation, both of which are required for the antidepressant behavioral actions of ketamine (2, 4). However, the initial cellular trigger for the rapid release of glutamate in the PFC and the antidepressant behavioral actions of ketamine remains unclear.

Two mechanistic hypotheses have been proposed for ketamine's initial cellular trigger (6, 7). The direct hypothesis posits that ketamine's antidepressant effects result from *direct* antagonism of NMDARs on principle-glutamatergic neurons causing homeostatic synaptic plasticity and increased synaptic drive. Alternatively, the indirect hypothesis, or disinhibition hypothesis, proposes that ketamine first inhibits GABAergic interneurons leading to the disinhibition of principle-glutamatergic neuron activity. During basal, resting state conditions, pyramidal cell firing is inhibited by presynaptic tonic firing GABA interneurons (8, 9). Because ketamine is an NMDAR open-channel blocker that requires activity to remove Mg²⁺ blocking entry to the channel, tonic firing GABA interneurons should be more sensitive to low, antidepressant doses of ketamine, resulting in a rapid disinhibition of pyramidal neurons and the subsequent

transient glutamate burst. Furthermore, as discussed in Homayoun & Moghaddam (2007) (10), fast-spiking GABAergic interneurons have faster excitatory postsynaptic potentials (EPSPs) than pyramidal neurons and are more effectively recruited by excitatory inputs (11, 12). These findings support earlier studies and suggest that NMDAR antagonists initially regulate the spontaneous firing of GABAergic interneurons to a greater extent than pyramidal neurons (8, 9). A recent study of hippocampal slices provides further support, demonstrating that ketamine reduces inhibitory input and disinhibits CA1 pyramidal neurons (13). Studies of GABA interneurons in depression have focused on the somatostatin (*Sst*) and parvalbumin (*Pvalb*) expressing subtypes, which together make up approximately 70 percent of GABA interneurons (14). These two subtypes innervate different aspects of excitatory neurons (*Sst*-dendrites, *Pvalb*-cell bodies) and have different electrophysiological properties (15).

NMDARs are a heterotetramer complex composed of two obligatory GluN1 subunits and two additional subunits that are a combination of GluN2A, GluN2B, GluN2C or GluN2D. Previous studies have demonstrated that a selective GluN2B negative allosteric modulator (Ro 25-6981) produces antidepressant behavioral effects as well as synaptic changes similar to ketamine in rodent models (2, 3, 16). In addition, clinical studies demonstrate that a single dose of another selective GluN2B negative allosteric modulator, CP-101,606, produces antidepressant actions in depressed patients (17). Here, we use a viral mediated shRNA knockdown strategy, as well as conditional deletion approach to target GluN2B subunits on different populations of cells in the mPFC and thereby determine their role in mediating ketamine's antidepressant behavioral effects. We combine electrophysiology, behavior and molecular techniques to determine whether GluN2B containing NMDARs on excitatory neurons or GABAergic interneurons in the mPFC are necessary for ketamine's antidepressant effects.

Results

Ketamine reduces inhibitory postsynaptic currents in mPFC

We first tested the influence of ketamine on spontaneous postsynaptic currents in layer V pyramidal neurons of mPFC (Figure 1). If ketamine preferentially acts at NMDARs on GABAergic interneuron, we would expect a reduction in the inhibitory tone or frequency of spontaneous inhibitory postsynaptic currents (sIPSCs). In order to record sIPSCs and spontaneous excitatory postsynaptic currents (sEPSCs) simultaneously, whole-cell patch clamp recordings were performed at a holding potential of -65 mV (the Cl⁻ reversal potential in the pipette solution is -72 mV). Spontaneous postsynaptic currents were determined before and during bath application of ketamine at 1 μ M, the estimated concentration reached in the human brain following i.v. infusion of a dose in the therapeutic range (18) and a concentration that blocks approximately 50% of NMDA-induced currents (19), or 10 μ M a concentration that is sufficient to block approximately 80% of NMDA-induced currents (20); these concentrations have also been used in recent reports (4, 13). The results demonstrate that 1 μ M ketamine significantly decreased sIPSC but increased sEPSC in both male and female mice (Figure 1A-D); the cumulative probability curves for interevent intervals are shifted to the right for sIPSCs (i.e., longer intervals, decreased frequency), while for sEPSCs the curves are shifted to the left (i.e., shorter intervals, increased frequency) (Figure 1C,D). Ketamine at 1 μ M increased sEPSC amplitude in both male and female mice, corresponding to increased sEPSC frequency; sIPSC amplitude was increased in males but decreased in females (the reason for this difference is unknown) (Supplemental figure 1E,F). In contrast, 10 μ M ketamine significantly decreased basal rates of both sIPSCs and sEPSCs in male and female mice (Supplemental Figure 1A-C). These findings are consistent with the hypothesis

that GABA interneuron-mediated IPSCs are more sensitive to ketamine blockade than glutamate pyramidal neuron-mediated EPSCs responses.

Knockdown of NMDAR-GluN2B on GABA but not glutamate neurons produces baseline antidepressant-like effects and occludes the actions of ketamine

First, we confirmed that glutamatergic pyramidal neurons and GABAergic interneuron subtypes in the mPFC express GluN2B using immunohistochemistry: GluN2B co-labelled with CaMKII (pyramidal cell) or glutamate decarboxylase 67 (GAD67; GABA interneuron) cells (labelled using specific antibodies) and *Sst*- or *Pvalb*-tdTomato+ cells (Supplemental Figure 2-A-D). Furthermore, bath application of the selective GluN2B antagonist conantokin G (2 μ M) reduced the NMDA-induced inward currents in pyramidal, *Sst*, and *Pvalb* cells in the mPFC (Supplemental Figure 3), demonstrating the expression of GluN2B subunits.

To target specific cell-types, we used a shRNA Mediated Adeno-associated virus (AAV) Cell type specific Knock-down (sMACK-down) approach, combining viral expression of shRNA targeting GluN2B with cell specific Cre-recombinase (Cre+) transgenic mouse lines. The GluN2BshRNA construct (Figure 2A) expresses both mCherry and EGFP and in the presence of Cre-recombinase, EGFP is deleted, resulting in expression of only mCherry (as a marker of recombination) and GluN2BshRNA. The GluN2BshRNA construct was packaged into an adeno-associated virus-2 (AAV2^{GluN2BshRNA}; Virovek). We confirmed that viral mediated GluN2BshRNA expression reduces GluN2B in a Cre-dependent manner in primary neuronal cultures (Figure 2B-D). Additionally, we confirmed cell specific viral-mediated knockdown of GluN2B significantly reduced the NMDA-, but not AMPA-induced inward currents in layer 5 pyramidal neurons in different lines of Cre recombinase transgenic mice used in this study, including *Camk2a-Cre*

(*Camk2a^{Cre+}*), *Gad1^{Cre+}*, *Sst^{Cre+}* and *Pvalb^{Cre+}* male mice as well as in *Sst^{Cre+}* female mice (Figure 2F-J). To identify interneurons for the slice electrophysiology experiments, *Sst-Td-Tomato* mice (for *Sst^{Cre+}*), *Pvalb-Td-Tomato* mice (for *Pvalb^{Cre+}*), or both *Pvalb-Td-Tomato* and *Sst-Td-Tomato* mice (for *Gad1^{Cre+}*) were used as controls.

Initial behavioral studies were conducted in *Camk2a^{Cre+}* mice to target principle neurons and in *Gad1^{Cre+}* mice to target all GABA interneuron subtypes. We also focused on male mice with a plan to extend the results to females once we identified which cell type was involved in the ketamine response. AAV2^{GluN2BshRNA} was infused bilaterally into mPFC (prelimbic and infralimbic regions) of *Camk2a^{Cre+}* and *Gad1^{Cre+}* adult (8-12 week) male mice and wild-type (WT), *Camk2a^{Cre-}* and *Gad1^{Cre-}* littermate controls (Figure 3A). The mPFC was targeted, as prior studies show that this region is necessary and sufficient for the antidepressant actions of ketamine (2, 21). Three weeks after viral infusion to allow for GluN2BshRNA expression and GluN2B knockdown, mice underwent behavioral testing and then brains were collected for histology. *Camk2a^{Cre+}* and *Gad1^{Cre+}* mice with AAV2^{GluN2BshRNA} infusions (referred to as *Camk2a^{Cre+/AAV}* and *Gad1^{Cre+/AAV}*, respectively) displayed different subsets of cells with mCherry only (Figure 3B,F), demonstrating cell-specific recombination and expression of the GluN2BshRNA construct in each transgenic line. In *WT-Camk2a^{Cre-/AAV}* and *WT-Gad1^{Cre-/AAV}* controls labeled neurons were yellow (i.e., both mCherry and EGFP), demonstrating there was no recombination as expected.

Baseline testing was conducted to evaluate immobility, referred to as preswim (before ketamine) as part of the forced swim test (FST, a measure of behavioral despair); in addition, preswim is often used as an initial stressor before testing antidepressants in this paradigm. Baseline behavior was also analyzed in an open field test (OFT), a measure of ambulatory activity (distance traveled), and anxiety behavior (time spent in center); the OFT also serves as an additional mild

stressor prior to ketamine treatment. One day after the OFT, mice were administered vehicle (saline, i.p.) or a single dose of ketamine (10 mg/kg, i.p.) and then tested 1 and 3 days later in the FST and novelty suppressed feeding test (NSFT, a measure of anxiety-like behavior), respectively. This dose of ketamine produces a rapid transient burst of glutamate and antidepressant behavioral responses (2-5, 15, 19) and the behavioral testing times (1 and 3 days) are used to avoid the acute locomotor and sensorimotor effects of ketamine administration and still show the rapid and sustained antidepressant effects of ketamine (Figure 3A). In *Camk2a^{Cre+/AAV}* male mice there were no differences in preswim immobility, or on center time or distance in the OFT (Figure 3C). Ketamine significantly decreased immobility in the FST in both *WT-Camk2a^{Cre-/AAV}* and *Camk2a^{Cre+/AAV}* mice (Figure 3D). In the NSFT, ketamine administration significantly reduced the latency to feed in both *WT-Camk2a^{Cre-/AAV}* and *Camk2a^{Cre+/AAV}* mice (Figure 3E). No significant differences were observed in home cage feeding (Figure 3E).

Using the same design, we found that *Gad1^{Cre+/AAV}* mice displayed significantly decreased baseline immobility in the preswim test, an antidepressant-like effect, compared with *WT-Gad1^{Cre-/AAV}* controls (Figure 3G); there were no significant effects on baseline behaviors in the OFT center time or total distance (Figure 3G). Saline treated *Gad1^{Cre+/AAV}* mice showed a significant baseline effect, similar to the pretest, and ketamine administration had no further effect beyond the baseline changes (Figure 3H). In *WT-Gad1^{Cre-/AAV}* controls, ketamine administration significantly decreased FST immobility time (Figure 3H). In the NSFT, ketamine treatment significantly reduced latency to feed compared to saline in the *WT-Gad1^{Cre-/AAV}* controls (Figure 3I). In *Gad1^{Cre+/AAV}* mice there was a nonsignificant decrease in baseline latency to feed, and the actions of ketamine were blocked or occluded (Figure 3I). No significant differences were observed in home cage feeding (Figure 3I). To address the possibility that GluN2B knockdown could produce

a floor effect on immobility, we treated a separate cohort of in *Gad1^{Cre+/AAV}* male mice with 20 mg/kg desipramine (DMI), a norepinephrine selective reuptake inhibitor (22). DMI administration significantly reduced immobility in the FST in both *WT-Gad1^{Cre-/AAV}* and *Gad1^{Cre+/AAV}* mice (Supplemental Figure 4).

Knockdown of GluN2B in *Sst* interneurons produces sex specific baseline behavioral effects and blocks the antidepressant-like effects of ketamine

To extend the results of the *Gad1^{Cre+}* study, we investigated the role of two major GABAergic interneuron subtypes, *Sst* and *Pvalb*, in the rapid antidepressant actions of ketamine (23). *Sst* and *Pvalb* interneurons display different molecular, electrophysiological, morphological, and circuit connectivity properties that could differentially contribute to the actions of ketamine (23). Postmortem studies of depressed subjects and rodent studies of chronic stress highlight a selective vulnerability of *Sst*-expressing GABAergic interneurons in PFC subregions (24, 25). We have reported that the initial cellular trigger for another rapid acting antidepressant, scopolamine, is dependent on *Sst*, but not *Pvalb*, interneuron M1-type muscarinic acetylcholine receptors (26). Based on these findings we initiated studies of *Sst* interneurons, including viral-mediated shRNA GluN2B knockdown and development of conditional deletion mutants (i.e., *Sst^{Cre+}Grin2b^{fl}*); we also compared male and female mice, and conducted electrophysiological and RNAseq studies.

Electrophysiology studies demonstrate that *Sst* interneurons are responsive to NMDA and that this effect is blocked by a selective GluN2B antagonist, conantokin G (Supplemental Figure 3); immunohistochemistry studies demonstrate that *Sst*⁺ interneurons in the mPFC express GluN2B (Supplemental Figure 2C,D). *Sst* GluN2B knockdown studies were carried out as described above. *Sst^{Cre+}* mice were infused with AAV2^{GluN2BshRNA} (*Sst^{Cre+/AAV}*) into the mPFC,

resulting in cell type-specific recombination (mCherry only, red cells), compared to *WT-SstCre-/AAV* control mice with no recombination (mCherry + EGFP double labeled yellow cells) (Figure 4A,B). Functional knockdown was also shown in *SstCre+/AAV* male and female mice by slice physiology, with decreased NMDA-, but not AMPA-induced inward currents (Figure 2H,I). In male *SstCre+/AAV* mice there was a significant decrease in immobility time in the preswim test compared to *WT-SstCre-/AAV* controls (Figure 4C); however, in female *SstCre+/AAV* mice there was no significant effect on immobility time (Figure 4C). There were no effects in male or female *SstCre+/AAV* mice in the OFT (4D,E). A single dose of ketamine significantly decreased FST immobility time in both male and female *WT-SstCre-/AAV* mice compared to saline controls (Figure 4F,I). In saline-treated *SstCre+/AAV* mice there was a significant decrease in baseline FST immobility in males and a trend for a decrease in females, and ketamine administration had no further effects in either sex (Figure 4F,I). In the NSFT, ketamine significantly reduced latency to feed in male and female *WT-SstCre-/AAV* mice when compared to saline controls but these effects were completely absent in *SstCre+/AAV* mice (Figure 4G,J). There was a small decrease in baseline latency to feed in female *SstCre+/AAV* mice, although this effect was not significant. No significant differences were observed in home cage feeding (Figure 4G,J). In males we also examined a reward-seeking behavior, the female urine sniffing test (FUST) (27). Male *WT-SstCre-/AAV* mice administered ketamine spent significantly more time sniffing female urine when compared to their genotype controls, and this effect was blocked in *SstCre+/AAV* mice (Figure 4H). There was no effect on baseline female urine sniffing time in male *SstCre+/AAV* mice, and no significant differences in time sniffing water across any group (Figure 4H).

To examine possible cellular determinants of the baseline behavioral differences in male and female *SstCre+/AAV* mice, we measured sIPSCs and sEPSCs layer V pyramidal neurons in

mPFC slices (Figure 4K-L). In *SstCre+/AAV* males there was a small but significant decrease in the frequency of sIPSCs, but a larger increase in sEPSCs (Figure 4K). In female *SstCre+/AAV* mice there was a significant decrease in the frequency of sIPSCs but no effect on sEPSCs (Figure 4L). The increase in basal sEPSCs in male mice could contribute to the baseline antidepressant-like effects observed in the preswim in male vs. female *SstCre+/AAV* knockdown mice (Figure 4C). Despite there being no significant difference in sEPSCs in female mice, there was still an occlusion of ketamine's effects in female *SstCre+/AAV* knockdown mice. These findings suggest there may be varying molecular and cellular profiles that account for the observed sex differences.

To further examine cellular differences between males and females we examined NMDAR subunit composition in *Sst* interneurons. *Sst*-tdTomato interneurons from mPFC were sorted by FACS and levels of NMDAR subunits determined by RNAseq. We found that expression of the GluN2B subunit, encoded by the *Grin2b* gene, in male and female mPFC is higher compared to *Grin2a*, similar to reports of *Grin2b* predominance in *Sst+* interneurons of adult male mouse visual cortex (28). In addition, there were no significant sex-specific differences in the expression of *Grin1*, *Grin2a* and *Grin2b* in *Sst+* interneurons (Supplemental Figure 5A-B). Since NMDAR channel opening requires AMPA receptor (AMPA) activity we also examined the relative abundance of AMPAR subunits 1 and 2, encoded by *Gria1* and *Gria2* genes, respectively. Here, we observed significantly higher levels of *Gria2* and a trend for higher levels of *Gria1* in female mice compared to male mice (Supplemental Figure 5C). Further studies are required to determine if differences in AMPAR expression contribute to the behavioral differences in males and females and if GluN2B knockdown alters the expression patterns of NMDAR and AMPAR subunits.

Because ketamine is a nonselective NMDAR channel blocker, we tested whether knockdown of another subunit, GluN2A, would influence the behavioral actions of ketamine. The

efficacy of AAV2^{GluN2A}shRNA was confirmed by Cre-dependent GluN2A knockdown in primary neuronal cultures (Supplemental Figure 6B-D). In male *Sst*^{Cre+} mice with infusion of AAV2^{GluN2A}shRNA into mPFC (*Sst*^{Cre+}/AAV2A) there was no significant effect on baseline immobility time in preswim compared to *WT-Sst*^{Cre-}/AAV2A control mice (Supplementary Figure 6F). Ketamine administration significantly decreased immobility time in the FST in both *WT-Sst*^{Cre-}/AAV-2A and *Sst*^{Cre+}/AAV-2A mice (Supplemental figure 6G). In the NSFT, ketamine administration significantly reduced the latency to feed in both *WT-Sst*^{Cre-}/AAV2A and *Sst*^{Cre+}/AAV2A mice (Supplemental Figure 6I). No significant differences were observed in locomotor activity or home cage feeding following ketamine administration (Supplemental Figure 6H,I).

Genetic deletion of *Grin2b* from *Sst*⁺ interneurons

In addition to the viral-mediated approach, we generated *Sst* interneuron specific *Grin2b* deletion mice by crossing *Sst*^{Cre+} and *Grin2b*^{fllox} mice (*Sst*^{Cre+}/*Grin2b*^{fl}) and littermate controls (*Sst*^{Cre-}/*Grin2b*^{fl}). Baseline immobility in the FST and anxiety-related behaviors in the OFT were tested in adult male and female mice (Figure 5A). Similar to viral-mediated knockdown of GluN2B from *Sst*⁺ interneurons in the mPFC, male, but not female *Sst*^{Cre+}/*Grin2b*^{fl} mice showed reduced immobility in the FST compared to controls (Figure 5C). There were no differences observed in the OFT (center time or distance traveled) in either sex (Figure 5D,E). In male *Sst*^{Cre+}/*Grin2b*^{fl} mice there was also a significant antidepressant-like effect (increased time sniffing) in the FUST compared to *Sst*^{Cre-}/*Grin2b*^{fl} controls (Figure 5F). In preliminary studies we found that both male and female *Sst*^{Cre+}/*Grin2b*^{fl} mice responded similarly to ketamine (Supplemental figure 7), so we used a mixed cohort of males and females (24 hours after dosing). Ketamine significantly reduced immobility time in the FST in *Sst*^{Cre-}/*Grin2b*^{fl} controls but not *Sst*^{Cre+}/*Grin2b*^{fl} deletion mutants (Figure

5G). Ketamine also significantly reduced latency to feed in NSFT in the *SstCre-Grin2bfl* controls but not *SstCre+Grin2bfl* deletion mice (Figure 6H).

To examine the effects of genetic *Grin2b* deletion on neuronal activity, postsynaptic currents were recorded from layer V pyramidal neurons of the mPFC (Figure 5I-J). *SstCre+Grin2bfl* males displayed significantly decreased sIPSCs but increased sEPSCs (Figure 5J), similar to in vitro incubation of PFC slices with 1 μ m ketamine (Figure 1C), whereas *SstCre+Grin2bfl* females displayed significant decreases of both sIPSCs and sEPSCs (Figure 5K). The increase in sEPSCs in male mice could contribute to the baseline antidepressant-like effects observed in male vs. female *SstCre+Grin2bfl* deletion mutant mice (Figure 5C).

Knockdown of GluN2B in *Pvalb* interneurons blocks or occludes the antidepressant-like effects of ketamine

To further examine GABAergic interneuron subtypes in the actions of ketamine and to compare with *Sst* results, we conducted GluN2B knockdown studies in *Pvalb* interneurons. Preliminary studies demonstrate that *Pvalb* interneurons are responsive to GluN2B containing NMDARs (blocked by conantokin G) (Supplemental Figure 3) and that *Pvalb*⁺ interneurons in the mPFC express GluN2B (Supplemental Figure 2C,D). Functional knockdown was also shown in *PvalbCre+/AAV* male mice by slice physiology, with decreased NMDA-, but not AMPA-induced inward currents (Figure 2J). Using the same design described above, male and female *PvalbCre+* or *WT-PvalbCre-* littermate controls were infused with AAV2^{GluN2BshRNA} (*PvalbCre+/AAV* or *WT-PvalbCre-/AAV*) (Figure 6A), resulting in cell specific recombination with a subset of mCherry only labeled cells (Figure 6B). In contrast, in *WT-PvalbCre-/AAV* mice labeled neurons were yellow (mCherry + GFP labeled interneuron), demonstrating that there was no recombination. In

Pvalb^{Cre+/AAV} male and female mice there was no difference in baseline preswim immobility or OFT behavior compared to *WT-Pvalb*^{Cre-/AAV} controls (Figure 6C-E). A single dose of ketamine significantly decreased immobility time in *WT-Pvalb*^{Cre-/AAV}, but not in *Pvalb*^{Cre+/AAV} male (Figure 6F) and female mice (Figure 6H). Interestingly, *Pvalb*^{Cre+/AAV} female mice given saline showed significantly reduced baseline immobility in the FST and there was no further effect of ketamine (Figure 6H); there was a similar trend for decreased immobility in saline treated *Pvalb*^{Cre+/AAV} males. In the NSFT, ketamine significantly reduced the latency to feed in male and female *WT-Pvalb*^{Cre-/AAV} control mice compared to saline (Figure 6G,I); in male and female *Pvalb*^{Cre+/AAV} mice there was no baseline effect in the NSFT and there were no significant differences following ketamine administration, although there was a trend for a decrease in males (Figure 6G,I). No differences were observed in home cage feeding (Figure 6G,I). Next, we measured sIPSCs and sEPSCs in layer V pyramidal neurons of mPFC slices from *Pvalb*^{Cre/AAV} mice (Supplemental figure 8). In *Pvalb*^{Cre+/AAV} males there was a significant decrease in the frequency of sIPSCs (Supplemental figure 8A,B). In contrast to *Sst*^{Cre+/AAV} male findings, we observed a small but significant decrease in the frequency of sEPSCs in *Pvalb*^{Cre+/AAV} males (Supplemental figure 8A,B).

Discussion

The results of the present study demonstrate that GluN2B knockdown in GABAergic interneurons (*Gad1*, *Sst* or *Pvalb*), but not *Camk2a*/glutamate neurons, occludes and/or blocks the antidepressant behavioral actions of ketamine (Table 1). The results also provide electrophysiological evidence that a low concentration of ketamine blocks NMDARs on GABA interneurons in mPFC, resulting in decreased inhibitory input and increased sEPSCs on layer V

principle neurons. Viral knockdown or genetic deletion of GluN2B on *Sst* interneurons produces a similar significant increase (disinhibition) of EPSCs, but only in male mice, which could account for the sex difference in baseline behaviors. Together these studies provide strong evidence in support of the disinhibition hypothesis that the initial trigger for ketamine is blockade of GluN2B containing NMDARs on GABAergic interneurons in the mPFC. The mPFC layer V principle neurons projects to cortical and subcortical brain regions implicated in depression-related behaviors, including the basolateral nucleus of the amygdala, which is necessary and sufficient for the rapid and long-lasting antidepressant actions of ketamine (19, 21). Because behavioral tests were conducted 24 hr after dosing to avoid the acute side effects of ketamine, we also acknowledge the possibility that there could be adaptations that require GluN2B on GABA interneurons that mediate the actions of ketamine.

An early *in vivo* electrophysiology study reported that ketamine administration resulted in blockade of GABA interneuron activity in the mPFC, which preceded an increase in glutamate neuronal activity, although the association between these two events could only be inferred (10). A recent *in vitro* electrophysiology study found that ketamine disinhibits CA1 pyramidal neurons in hippocampal slices, in agreement with the disinhibition hypothesis (13). Here we show that a low concentration of ketamine (1 μ M), which approximates brain levels after an antidepressant dose of ketamine (18), decreases sIPSCs but increases sEPSCs of layer V pyramidal neurons in male and female mice, consistent with the hypothesis that ketamine blocks NMDARs on tonic firing GABAergic interneurons, decreasing inhibitory inputs onto excitatory pyramidal neurons. An interesting observation from these experiments is that female mice have more clustered high-frequency IPSCs compared to males, possibly due to a greater number and/or excitation of burst firing interneurons in females (29); however, additional studies are needed to address these

differences. In contrast, a higher concentration of ketamine (10 μ M) significantly decreased both sIPSCs and sEPSCs in layer V mPFC neurons of male and female mice, demonstrating the selective effect of the lower, 1 μ M concentration on sIPSCs.

To identify the subunit type and cellular localization of NMDARs underlying the antidepressant action of ketamine, we designed and validated a viral-mediated, Cre recombinase strategy (AAV2^{GluN2BshRNA}) to knockdown GluN2B or GluN2A on specific populations of neurons in the mPFC, a region that is necessary and sufficient for the actions of ketamine (2, 21). The GluN2B subunit was targeted based on evidence that selective GluN2B antagonists produce rapid antidepressant actions in depressed patients and rodent models (3, 16, 17). The results demonstrate that knockdown of GluN2B on *Gad1*/GABA interneurons, but not *Camk2a*/pyramidal neurons in the mPFC blocks and/or occludes the antidepressant-like behavioral effects of ketamine (Table 1). GluN2B knockdown on *Gad1*/GABA interneurons also produces baseline antidepressant-like effects on immobility in the preswim test, as well as the FST, a measure of behavioral despair, and occluded any further action of ketamine. To determine whether the occlusion of the ketamine response was due to a floor effect, we tested whether GluN2B knockdown in *Gad1*^{Cre+} mice also occluded the response to another antidepressant, DMI, which has a completely different mechanism (i.e., selective inhibition of norepinephrine reuptake). DMI administration produced a significant antidepressant effect in the FST in the *Gad1*^{Cre+} mice, demonstrating that there is not a floor effect that occludes the response to ketamine. These baseline effects suggest that GluN2B knockdown in *Gad1*^{Cre+} mice reduces NMDAR drive of GABA interneurons, similar to ketamine. The reason for the differential baseline effects in the FST and NSFT are unknown but could result from different cellular or circuit mechanisms that contribute to each behavior. Nevertheless, these results demonstrate a requirement for GluN2B on GABA interneurons in the actions of ketamine.

Our results of GluN2B knockdown in *Camk2a*/pyramidal neurons differ from a previous study by Hall and colleagues reporting that genetic deletion of *Grin2b* using a different excitatory neuron promoter (NEX or Neuro6d) produced baseline antidepressant effects in the FST that occluded the actions of ketamine (30). However, the NEX-Cre+ x *Grin2b* deletion mutant mice display 3-fold higher levels of locomotor activity than WT controls (31), which could very likely mediate the decreased baseline immobility and occlusion of the ketamine response in the FST (30). We did not observe any changes in locomotor activity in our viral *Camk2a*^{Cre+/AAV} or *Gad1*^{Cre+/AAV} knockdown mice, or in any other lines tested. Another study by Hall and colleagues used a viral approach to delete *Grin2b* from pyramidal neurons in the mPFC (*Grin2b*^{Floxed} mice plus AAV-*Camk2a* driven Cre recombinase), reporting decreased baseline immobility time in the FST (32); the influence of ketamine was not examined in this study. The reason for this baseline difference is not clear but could be due to the complete deletion of *Grin2b* in excitatory neurons and targeting of prelimbic PFC, as infralimbic, but not prelimbic PFC is required for the antidepressant actions of ketamine (21).

We next examined GABA interneuron subtypes, with a focus on *Sst* interneurons based on evidence from human postmortem studies reporting selective loss of *Sst*-interneurons in the PFC of depressed subjects (24, 25), and our previous studies of scopolamine (26). *Sst* interneurons can be regular-spiking, low threshold spiking, and burst firing (15), and blockade of these responses could underlie ketamine-mediated disinhibition. We found that either viral knockdown of GluN2B in the mPFC of *Sst*^{Cre+/AAV} or constitutive knockout of GluN2B in *Sst*^{Cre+Grin2bfl} mice occludes and/or blocks the antidepressant behavioral effects of ketamine in males and females (Table 1). In contrast, knockdown of GluN2A, another prominent subunit in cerebral cortex, on *Sst* interneurons did not block the antidepressant effects of ketamine, demonstrating specificity for GluN2B in the

actions of ketamine (Table 1). Finally, in both viral knockdown and genetic deletion mutant mice we observed that removal of GluN2B from *Sst* interneurons produced a significant decrease in preswim immobility in male mice only, indicating a sex-specific role for *Sst* interneurons in this baseline behavior effect.

Electrophysiological studies of the sex differences show that GluN2B knockdown in *SstCre+/AAV* or deletion in *SstCre+Grin2bfl* mice significantly increased sEPSCs in layer V pyramidal neurons of males, demonstrating an association with antidepressant behavior that was not observed in females. These findings indicate that removal of GluN2B subunits from *Sst* interneurons results in disinhibition of the pyramidal cells, similar to the effects of ketamine. In support of this hypothesis, one study reported that optogenetic inhibition of *Sst* interneurons increases action potential firing and burst firing in nearby excitatory neurons in the barrel cortex (33). Why this is not observed in females is unknown, but could be due to different NMDAR and/or AMPAR expression, or synaptic alterations that counter the effects of GluN2B knockdown. Analysis of NMDAR and AMPAR subunit expression revealed no significant sex differences in relative abundance of *Grin1*, *Grin2a* or *Grin2b* in *Sst+* interneurons, but significantly greater expression of *Gria2* in females compared to males. Increased *Gria2* in female mice could be sufficient to maintain higher tonic firing of *Sst+* interneurons and inhibitory control of glutamatergic neurons upon knockdown or deletion of *Grin2b*. Sex differences in NMDAR and/or AMPAR expression on excitatory neurons, which are known to be influenced by estrogen, could also contribute to the observed behavioral effects in males and females (34, 35). Female rats have higher baseline PFC GluN1 expression and increased stress-induced expression of GluN2B compared to males (36). Postmortem studies report that female depressed subjects had increased expression of several glutamate receptor subtypes in the dorsolateral PFC, and that female depressed-suicide subjects

had significantly increased expression of *Grin2b* (37). Only one study to date has analyzed sex-differences in ketamine response and found no differences in efficacy or tolerability (38, 39). These studies highlight the need for further studies of sex differences in the behavioral, neural, molecular and genetic phenotypes of MDD to inform the development of more effective treatment options (40).

Pvalb interneurons are noted for their fast-spiking properties at rest, and could also be involved in ketamine-mediated disinhibition(15). We found that viral knockdown of GluN2B in the mPFC of *Pvalb^{Cre+}/AAV* male and female mice blocked the antidepressant behavioral effects of ketamine (Table 1). This differs from our previous study of scopolamine where we found that knockdown of M1-AChR on *Sst*, but not *Pvalb*, interneurons blocked the antidepressant effects of scopolamine (26), raising the possibility that the disinhibition resulting from the actions of ketamine on both *Sst* and *Pvalb* interneurons contributes to its greater therapeutic efficacy relative to scopolamine (41). Indeed, animals that have been subjected to inescapable footshock have reduced excitatory drive onto prefrontal *Pvalb* interneurons and chemogenetic activation of these interneurons can lead to susceptibility in resilient mice, suggesting *Pvalb* interneurons are also important in regulating depression-like behavioral output (42). Saline treated *Pvalb^{Cre+}/AAV* mice displayed decreased immobility, which could result from blockade of increases that are observed with repeated swim exposure that is observed in rodents, suggesting a role for GluN2B subunits on mPFC *Pvalb* interneurons in memory or stress resiliency processes. For example, blocking synaptic transmission in mPFC *Pvalb* interneurons impairs spatial working memory and reversal learning but has no effect on anxiety as measured by the OFT (43). A previous study reported that constitutive global genetic deletion of *Grin1* from *Pvalb^{Cre+}* mice did not block the effects of

ketamine (44). The differences in the scope and developmental targeting of *Grin1* deletion in *Pvalb* interneurons could underlie the different behavioral outcomes in these studies.

The results of the current study provide direct evidence that the initial cellular trigger for the antidepressant actions of ketamine is blockade of NMDARs on GABAergic interneurons, not excitatory neurons, leading to disinhibition and a burst of glutamate that drives synaptic and behavioral responses. Ketamine blockade of GABA activity appears to be in opposition to evidence of a reduction of GABA, particularly *Sst* interneurons, in depression (24, 25). Our results also appear to contradict rodent studies reporting that increased *Sst* interneuron function produces antidepressant behavioral responses (45). However, ketamine blockade of NMDARs and the resulting glutamate burst are transient, returning to baseline levels by 80 min after dosing (5), but lead to the long-lasting synaptic and antidepressant behavioral actions (2, 22, 46, 47). In addition, recent work reports that a single dose of ketamine also leads to increased GABA function in the mPFC 24 h after dosing, evidence of further adaptations to the initial glutamate burst that would contribute to correction of GABA, as well as glutamate deficits (48). This could also explain the apparent contradictory effects reported in another rodent study, which found that repeated ketamine administration increased *Pvalb* interneuron activity in juvenile stressed mice (49), but this likely represents an adaptation to repeated induction of the glutamate burst. Thus, the impact of transient vs. sustained effects are critical when interpreting these experiments.

In conclusion, conventional monoaminergic antidepressant treatments take weeks to months to produce a therapeutic response and are ineffective for treatment resistant depression. The novel, rapid-acting antidepressant actions of ketamine are effective even for patients considered treatment resistant, but the abuse potential of ketamine remains a limitation. Dissection of the cellular and molecular mechanisms underlying ketamine's antidepressant effects could lead

to the development of more targeted and safer treatments for depression. The results of the current study reveal an important cellular mechanism by which ketamine produces rapid antidepressant actions, indicating that activity related neurotransmitter receptors and channels on *Sst* and *Pvalb* interneurons in the mPFC are promising targets for the development of novel rapid-acting antidepressants.

Methods

Animals. For electrophysiology experiments looking at the effects of ketamine, wild-type C57BL/6 male and female mice were used (Jackson Laboratories). For electrophysiology experiments looking at the effects of ketamine or conantokin G on NMDA-induced inward currents, wild-type C57BL/6 (Jackson Laboratories), *Sst*-tdTomato, or *Pvalb*-tdTomato male mice were used. To obtain *Sst*- and *Pvalb*-tdTomato mice, *Sst-Cre* and *Pvalb-Cre* mice were bred with Ai9(RCL-tdT) mice (catalog 007909), all from Jackson Laboratories. For FACs and RNA-sequencing, *Sst-tdTomato* male and female mice were used. For viral studies, male and female transgenic mice and WT C57BL/6 littermates were obtained from in-house breeders. *Gad1-Cre* mice were originally obtained from Marina Picciotto (50), and *Camk2a-Cre* mice were obtained from Günter Schütz (German Cancer Research Center, Heidelberg, Germany) (51). *Pvalb-Cre* (catalog 008069) and *Sst-Cre* (catalog 013044) mice were obtained from Jackson Laboratories. *Grin2B^{flox}/Sst-Cre⁺* mice were produced by crossing *Grin2b* floxed mice (Dr. Eric Delpire, Vanderbilt University) (52) with *Sst-Cre* heterozygous mice to produce *Grin2B^{flox}/Sst-Cre⁺* and *Grin2B^{flox}/Sst-Cre⁻* offspring. For lines that required additional breeding, at least 6 backcrosses were performed. All studies were performed with adult mice. Pregnant female rats were used as a source of embryonic tissue for primary neuronal cultures (Jackson Laboratories).

Animals were housed in standard ventilated rack under a 12-hour light/12-hour dark cycle with ad libitum access to water and rodent chow. All experiments were performed during the 12-hour light cycle. Animal use and procedures were in accordance with the National Institutes of Health guidelines and approved by the Yale University Animal Care and Use Committees.

Brain slice electrophysiology. Brain slices containing the mPFC were prepared from male and female mice (8 to 16 weeks old). Brains were placed in artificial cerebrospinal fluid (ACSF) (pH 7.35–7.38) equilibrated with 95% O₂/5% CO₂. Coronal slices of 300- μ m thickness containing the mPFC were transferred to the fixed stage of an Olympus BX50WI scope for whole-cell recording. The chamber was continuously perfused with normal ACSF at a rate of 2 to 3 ml/min and its temperature maintained at $33 \pm 0.5^\circ\text{C}$. Patch pipettes (3–5 M Ω) were pulled from glass tubing with a Flaming-Brown Horizontal Puller. The pipette solution contained the following: 115 mM K gluconate, 5 mM KCl, 2 mM MgCl₂, 2 mM Mg-ATP, 2 mM Na₂ATP, 10 mM Na₂-phosphocreatine, 0.4 mM Na₂GTP, and 10 mM HEPES, pH 7.33. Neurons were visualized by videomicroscopy using microscope (40x IR lens) with infrared differential interference contrast (IR/DIC). Whole-cell recordings were made with an Axoclamp-2B amplifier. Postsynaptic currents were studied in the continuous single-electrode voltage-clamp mode (3000 Hz low-pass filter). Spontaneous inhibitory postsynaptic currents (sIPSCs) and spontaneous excitatory postsynaptic currents (sEPSCs) were simultaneously recorded (53–55) at a holding potential of -65 mV. Because the reverse potential of Cl⁻ is -72mV (calculated from pipette solution), at -65mV membrane potential, sIPSCs and sEPSCs were distinguished by their outward and inward polarity, respectively. Synaptic events were analyzed using Mini Analysis Software (Synaptosoft, Leonia, NJ). NMDA (10 μ m)- and AMPA (5 μ m) -induced inward currents were tested with no added magnesium in the ACSF.

Immunohistology. After 3 weeks to allow for viral expression, brains were collected from mice infused with AAV2GluN2BshRNA after transcardiac perfusion with sterile PBS and 4% paraformaldehyde (PFA). Brains were post-fixed in 4% PFA for 24 hours and incubated in 30% sucrose for an additional 24 hours. Fixed brains were frozen and sectioned at 30uM using a Microm HM550 cryostat. To examine the colocalization of GluN2B with different cell markers, brain sections were washed and incubated with blocking buffer (PBS+0.3% TritonX-100+4% normal goat serum; 1hr at room temperature) followed by overnight incubation with primary antibodies at 4°C: anti-Camk2a (Enzo Life Sciences, catalog no. KAM-CA002-D, 1:1000, Rat), anti-GAD67 (Sigma-Aldrich, catalog no. G5419, 1:1000, Mouse) and anti-GluN2B (EMD Millipore, catalog no. AB1557, 1:500, Rabbit). Brain sections from *Sst-tdTomato* and *Pvalb-tdTomato* reporter mice were used for immunolabeling of GluN2B on *Sst+* and *Pvalb+* interneurons (anti-GluN2B, Alomone Labs, catalog no. AGC-003, 1:200, Rabbit). To match the style of *Camk2a* and GAD67 images, *Sst+* and *Pvalb+* stains were flipped to green and GluN2B stains were flipped to red. Sections were then washed and incubated overnight at 4°C or 2hr at room temperature with fluorescent conjugated secondary antibodies (Alexa Fluor, ThermoFisher Scientific, 1:1,000 dilution). Immunofluorescence was visualized using a confocal laser scanning microscope (Olympus FV1000).

shRNA and viral preparation. For knockdown of GluN2B or GluN2A in specific neuronal cell types, an shRNA sequence was designed targeting the GluN2B or GluN2A subunit (56). GluN2B shRNA
(5'-TgtaccaacaggtctcaccttaaacTTCAAGAGAgtttaaggtgagacctgttggtacTTTTTTC-3') or GluN2A shRNA

(5'-TtgacagaacgcgaacttcgaaatcTTCAAGAGAgatttcgaagttcgcggttctgtcaTTTTTTC-3'; Integrated DNA Technologies) was ligated into a plasmid (pGluN2BshRNA or pGluN2AshRNA) designed to restrict shRNA expression to cells that express Cre recombinase (57). The TATAloxP-flanked CMV-EGFP cassette was subcloned from pSico (from Tyler Jacks, Massachusetts Institute of Technology, Boston, Massachusetts, USA; Addgene plasmid catalog 11578) into pAAV-mCherry (Virovek) to generate the sMACK-down backbone. This plasmid allows ubiquitous mCherry expression and conditional EGFP expression driven by floxed CMV cassette that prevents shRNA expression with U6 promoter disruption.

Primary Cortical Cultures. Pregnant female rats were euthanized and cortices from E18 embryos were dissected. Following incubation in trypsin-EDTA (0.25%, Gibco) for 10 min, cortices were dissociated and neurons were plated at 1 million cells per well in 6-well poly-D-lysine-coated plates in DMEM (Gibco)/10% FBS (fetal bovine serum). Medium was changed the following day to a serum-free medium containing neurobasal and B27 (Gibco) which was changed every 4 days. Cells were maintained at 37 °C, 5% CO₂, and 95% humidity. At day in vitro (DIV) 5, 0.4 uL AAV2^{GluN2BshRNA} OR AAV2^{GluN2AshRNA}, AAV1-Cre, or both viruses in combination were added to the wells. After 21 days (DIV26) of viral infection and shRNA expression, cells were collected for western blot analysis.

Western blot analysis. Levels of GluN2B or GluN2A from cell lysates were analyzed by western blot analysis. Cells were collected into RIPA lysis buffer containing 50 mM Tris-HCl (pH 7.5), 150 mM NaCl, 1% Triton X-100, 0.1% SDS, 1 mM NaVO₃, 5 mM NaF and 1×protease inhibitor cocktail. Homogenates were then centrifuged at 13,000 rpm for 10 min to remove cell debris. The supernatant was collected and total protein concentrations measured using a protein assay kit (Pierce BCA Protein Assay Kit, Thermo Scientific, USA). Twenty µg of protein were

electrophoretically separated on an SDS-PAGE gel (7.5% Tris-HCL) and transferred to 2 μ m Polyvinylidene fluoride or polyvinylidene difluoride (PVDF) membranes. Membranes were blocked with 5% BSA in PBS+0.05% Tween 20 (PBS-T) and then incubated with GluN2B antibody (Ab) (Cell Signaling, catalog no. 4307, 1:1000; Rabbit) or GluN2A Ab (BD biosciences, catalog no. 612286, 1:1000, Mouse) overnight. Membranes were then washed in PBS-T (3x for 10 min each) and incubated in peroxidase labeled anti-rabbit (Vector laboratories, catalog no. PI-1000, 1:10,000) or anti-mouse secondary (Cell Signaling, catalog no. 7076, 1:10,000) at room temperature for 1 hour. Protein bands were analyzed using enhanced chemiluminescence (ECL). After detection of GluN2B or GluN2A, membranes were incubated in stripping buffer (Thermo Scientific), blocked in 5% BSA in PBS-T for 1 hour and then reprobred with beta-actin (Cell Signaling, catalog no. 4970, 1:1000) overnight. Densitometry was used to quantify protein bands (Image Lab, BioRad) and GluN2B or GluN2A was normalized to their respective beta-actin level (loading control).

Surgery and cortical infusion. Mice were anesthetized with a ketamine/xylazine (100/10 mg/kg) cocktail. Bilateral viral infusions into the mPFC (0.5 μ l per side; 0.1 μ l/minute) were performed with coordinates (from bregma) as follows: +2.0 mm anterior-posterior, \pm 0.4 mm medial-lateral, and -2.8 mm dorsal-ventral (58). Incisions were closed with sutures, and an antibiotic was applied to prevent infection. Mice received i.p. injection of carprofen (5 mg/kg) immediately after surgery and daily for the next 2 days.

Drug administration. For ketamine experiments, mice received 1 injection of vehicle (0.9% saline) or ketamine (10 mg/kg, i.p.) 24-hours before behavioral testing. For desipramine experiments, mice received 1 injection of vehicle (0.9% saline) or desipramine (20 mg/kg, i.p.) 30-minutes before behavioral testing.

Open field test (OF). The OFT was conducted in a Plexiglas test apparatus (40 × 40 × 25 cm) and recorded for 10 minutes. Activity in the open field test was analyzed using an automated system (ANY-maze, Stoelting).

Forced Swim Test (FST). FST, referred to as preswim if administered prior to drug treatment, was conducted as previously described (2). Mice were placed for 6 minutes in a clear cylinder filled with water (24 ± 1 °C, 18 cm depth). Sessions were video recorded and scored for total immobility time by a blinded experimenter. Time immobile during the 2- to 6-minute block is reported.

Novelty-Suppressed Feeding Test (NSFT). NSFT was conducted as previously described (59). Mice were food deprived for 18 hours and placed in a dimly lit box (40 × 40 × 25 cm) with food in the center. The latency to feed was recorded. Home cage food intake over a 15-minute period was measured as a feeding control.

RNA preparation and RNA-sequencing. In brief, the mPFC was dissected from *Sst-tdTomato* reporter mice and incubated in DMEM (GIBCO)/0.25% trypsin (GIBCO) for 30 min at 37°C. The tissue pieces were then homogenized using a 20% FBS/HBSS/0.2% BSA solution, centrifuged (1200xg for 6 min) to collect the cells and resuspended and filtered using HBSS/0.2% BSA solution. Fluorescent cells were sorted and collected into 100 µL of lysis buffer (Norgen kit) using fluorescence activated cell sorting (FACSCalibur, Becton Dickson). RNA was extracted using Arcturus PicoPure RNA isolation kit (Applied Biosystems). 100 ng of total mRNA was processed using the Pico RiboGone-Mammalian (TakaraBio, Kyoto, Japan) before cDNA synthesis. RNA-sequencing was performed on an Illumina HiSeq2500 using 75-bp, paired-end sequencing. FASTQ files were trimmed and assessed for quality control before being annotated with the mouse genome (mm9) using TopHat241. The assembled transcripts were used to estimate transcript

abundance and Fragments Per Kilobase of transcript per Million mapped reads (FPKM) values using cuffdiff42 and R (The Comprehensive R Archive Network. Cran.R-Project.org). RNA seq data was deposited to NCBI GEO data set repository (GEO accession# GSE138670).

Female urine sniffing test (FUST). This test was conducted according to previously published procedures (27). Male mice were habituated for 60 min to a sterile cotton-tipped applicator placed in their home cage. For the test, mice were first exposed to a new cotton tip dipped in sterile water; 45 min later, mice were then exposed to another cotton tip infused with 45 uL fresh urine collected from adult females of the same strain. Estrous cycle was not measured as prior studies have reported that females in all states of estrus elicit higher investigation from males than ovariectomized females (60). Behavior was video recorded for 5 minutes per test and total time spent sniffing the cotton-tipped was determined. Time spent biting the cotton-tip was excluded from the recording time.

Locomotor Activity (LMA). Animals were placed in a clean testing cage (30 cm × 19 cm × 13 cm) for 30 min, during which the number of beam breaks was measured using the Med-PC software (Med Associates, St Albans, VT).

Statistics. Data were subjected to statistical analyses with GraphPad Prism 8. The results are expressed as the mean ± standard error of mean (S.E.M.). Statistical significance was determined by a one-way analysis of variance (ANOVA) or a two-way ANOVA, followed by the Tukey's or Sidak's (FUST) multiple comparison test for comparing the treated group with the control group and multi-group comparisons as indicated in the figure legends. Statistical differences between any two groups were determined using either the Student's two-tailed t-test or Kolmogorov–Smirnov two-sample test. Across all analyses, differences were considered significant if $P < 0.05$. Any value greater than 2 times the standard deviation of the mean was considered an outlier and

removed from further analysis of the test at hand. The specific test used for each figure is mentioned in the figure legend. Each experiment was conducted a minimum of two times.

Study approval. Animal use and procedures were in accordance with NIH guidelines and approved by the Yale University Animal Care and Use Committees.

Author Contributions

D.M.G, S.P., E.S.W, and R.S.D. designed the study. D.M.G., S.P., R.J., M.W, M.J.G, and C.H.D. conducted experiments, analyzed data and interpreted the results. X-Y.L. helped with breeding, genotyping and the development of the *SstCre+Grin2bfl* mouse line. S.R.T. and M.R.P. contributed essential reagents and experimental advice for cell type-selective knock down experiments. E.D. provided the *Grin2b^{lox}* line and helped with the design of the *Grin2b^{lox}* lines used in the study. D.M.G. and R.S.D. wrote the manuscript. D.M.G. was designated as the first co-first author based on primary contributions. All authors reviewed and approved the final manuscript.

Acknowledgements

This research was supported by National Institute of Mental Health grants MH093897 and MH105910 (R.S.D) and the State of Connecticut. SRT and MRP were supported by DA14241 and MH077681. The *Glun2b^{lox}* mouse was generated by the Gene-Targeted Mouse Core of the INIA-stress consortium (grant U01 AA013514 to E.D.).

References

1. Berman RM, et al. Antidepressant effects of ketamine in depressed patients. *Biol Psychiatry*. 2000;47(4):351-4.
2. Li N, et al. mTOR-dependent synapse formation underlies the rapid antidepressant effects of NMDA antagonists. *Science* 2010;329(5994):959--64.

3. Li N, et al. Glutamate N-methyl-D-aspartate receptor antagonists rapidly reverse behavioral and synaptic deficits caused by chronic stress exposure. *Bio Psychiatry*. 2011;69(8):754--61.
4. Autry AE, et al. NMDA receptor blockade at rest triggers rapid behavioural antidepressant responses. *Nature*. 2011;475(7354):91--5.
5. Moghaddam B, et al. Activation of glutamatergic neurotransmission by ketamine: a novel step in the pathway from NMDA receptor blockade to dopaminergic and cognitive disruptions associated with the prefrontal cortex. *J Neurosci*. 1997;17(8):2921--7.
6. Gerhard DM, et al. *Drug Discov Today*. 2016:454--64.
7. Miller OH, et al. *Neuropharmacology*. 2016:17--26.
8. Constantinidis C, and Goldman-Rakic PS. Correlated discharges among putative pyramidal neurons and interneurons in the primate prefrontal cortex. *J Neurophysiol*. 2002;88(6):3487--97.
9. Rao SG, et al. Isodirectional tuning of adjacent interneurons and pyramidal cells during working memory: evidence for microcolumnar organization in PFC. *J Neurophysiol*. 1999;81(4):1903--16.
10. Homayoun H, and Moghaddam B. NMDA receptor hypofunction produces opposite effects on prefrontal cortex interneurons and pyramidal neurons. *J Neurosci*. 2007;27(43):11496--500.
11. Kawaguchi Y. Distinct firing patterns of neuronal subtypes in cortical synchronized activities. *J Neurosci*. 2001;21(18):7261--72.
12. Povysheva NV, et al. Properties of excitatory synaptic responses in fast-spiking interneurons and pyramidal cells from monkey and rat prefrontal cortex. *Cereb Cortex*. 2006;16(4):541--52.
13. Widman AJ, and McMahon LL. Disinhibition of CA1 pyramidal cells by low-dose ketamine and other antagonists with rapid antidepressant efficacy. *Proc Natl Acad Sci U S A*. 2018;115(13):E3007--E16.
14. DeFelipe J, et al. New insights into the classification and nomenclature of cortical GABAergic interneurons. *Nat Rev Neurosci*. 2013;14(3):202--16.
15. Tremblay R, et al. GABAergic interneurons in the neocortex: From cellular properties to circuits. *Neuron*. 2016;91(2):260--92.
16. Maeng S, et al. Cellular mechanisms underlying the antidepressant effects of ketamine: role of alpha-amino-3-hydroxy-5-methylisoxazole-4-propionic acid receptors. *Biol Psychiatry*. 2008;63(4):349--52.
17. Preskorn SH, et al. An innovative design to establish proof of concept of the antidepressant effects of the NR2B subunit selective N-Methyl-D-Aspartate antagonist, CP-101,606, in patients with treatment-refractory major depressive disorder. *J Clin Psychopharmacol*. 2008;28(6):631--7.
18. Hartvig P, et al. Central nervous system effects of subdissociative doses of (S)-ketamine are related to plasma and brain concentrations measured with positron emission tomography in healthy volunteers. *Clin Pharmacol Ther*. 1995;58(2):165--73.
19. Hare BD, et al. Optogenetic stimulation of medial prefrontal cortex Drd1 neurons produces rapid and long-lasting antidepressant effects. *Nat Commun*. 2019;10(1):223.
20. Halliwell RF, et al. The mechanism of action and pharmacological specificity of the anticonvulsant NMDA antagonist MK-801: a voltage clamp study on neuronal cells in culture. *Br J Pharmacol*. 1989;96(2):480--94.

21. Fuchikami M, et al. Optogenetic stimulation of infralimbic PFC reproduces ketamine's rapid and sustained antidepressant actions. *Proc Natl Acad Sci U S A*. 2015;112(26):8106-11.
22. Duman RS, et al. Synaptic plasticity and depression: new insights from stress and rapid-acting antidepressants. *Nat Med*. 2016;22(3):238--49.
23. Markram H, et al. Interneurons of the neocortical inhibitory system. *Nat Rev Neurosci*. 2004;5(10):793--807.
24. Seney ML, et al. Laminar and cellular analyses of reduced somatostatin gene expression in the subgenual anterior cingulate cortex in major depression. *Neurobiol Dis*. 2015;73:213--9.
25. Lin LC, and Sibille E. Somatostatin, neuronal vulnerability and behavioral emotionality. *Mol Psychiatry*. 2015;20(3):377--87.
26. Wohleb ES, et al. GABA interneurons mediate the rapid antidepressant-like effects of scopolamine. *J Clin Invest*. 2016;126(7):2482--94.
27. Malkesman O, et al. The female urine sniffing test: A novel approach for assessing reward-seeking behavior in rodents. *Biol Psychiatry*. 2010;67(9):864--71.
28. Tasic B, et al. Adult mouse cortical cell taxonomy revealed by single cell transcriptomics. *Nat Neuro*. 2016;19(2):335--46.
29. Wang Y, et al. Anatomical, physiological and molecular properties of Martinotti cells in the somatosensory cortex of the juvenile rat. *J Physiol*. 2004;561(1):65--90.
30. Miller OH, et al. GluN2B-containing NMDA receptors regulate depression-like behavior and are critical for the rapid antidepressant actions of ketamine. *eLife*. 2014;3.
31. Wang C-C, et al. A critical role for GluN2B-containing NMDA receptors in cortical development and function. *Neuron*. 2011;72(5):789--805.
32. Miller OH, et al. Synaptic regulation of a thalamocortical circuit controls depression-related behavior. *Cell Rep*. 2017;20(8):1867--80.
33. Gentet LJ, et al. Unique functional properties of somatostatin-expressing GABAergic neurons in mouse barrel cortex. *Nat Neuro*. 2012;15(4):607--12.
34. Smith CC, et al. Estradiol and the relationship between dendritic spines, NR2B containing NMDA receptors, and the magnitude of long-term potentiation at hippocampal CA3-CA1 synapses. *Psychoneuroendocrinology*. 2009;34(SUPPL. 1):S130--S42.
35. Galvin C, and Ninan I. Regulation of the mouse medial prefrontal cortical synapses by endogenous estradiol. *Neuropsychopharmacology*. 2014;39(9):2086--94.
36. Wang Y, et al. Prenatal chronic mild stress induces depression-like behavior and sex-specific changes in regional glutamate receptor expression patterns in adult rats. *Neuroscience*. 2015;301:363--74.
37. Gray AL, et al. Sex differences in glutamate receptor gene expression in major depression and suicide. *Mol Psychiatry*. 2015;20(9):1057--68.
38. Freeman MP, et al. Sex differences in response to ketamine as a rapidly acting intervention for treatment resistant depression. *J Psychiatr Res*. 2019;110:166--71.
39. Gerhard DM, and Duman RS. Rapid-acting antidepressants: Mechanistic insights and future directions. *Curr Behav Neurosci Rep*. 2018;5(1):36--47.
40. Wickens MM, et al. Sex differences in psychiatric disease: A focus on the glutamate system. *Front Mol Neurosci*. 2018;11(197):1--12.

41. Park L, et al. Neurophysiological changes associated with antidepressant response to ketamine not observed in a negative trial of scopolamine in major depressive disorder. *Int J Neuropsychopharmacol*. 2019;22(1):10--8.
42. Perova Z, et al. Depression of excitatory synapses onto parvalbumin interneurons in the medial prefrontal cortex in susceptibility to stress. *J Neurosci*. 2015;35(7):3201--6.
43. Murray AJ, et al. Parvalbumin-positive interneurons of the prefrontal cortex support working memory and cognitive flexibility. *Sci Rep*. 2015;5(1):16778.
44. Pozzi L, et al. Mice lacking NMDA receptors in parvalbumin neurons display normal depression-related behavior and response to antidepressant action of NMDAR antagonists. *PLoS ONE*. 2014;9(1):e83879.
45. Fuchs T, et al. Disinhibition of somatostatin-positive GABAergic interneurons results in an anxiolytic and antidepressant-like brain state. *Mol Psychiatry*. 2017;22(6):920--30.
46. Ota KT, et al. REDD1 is essential for stress-induced synaptic loss and depressive behavior. *Nat Med*. 2014;20(5):531-5.
47. Duman RS, et al. Altered connectivity in depression: GABA and glutamate neurotransmitter deficits and reversal by novel treatments. *Neuron*. 2019;102(1):75--90.
48. Ghosal S, et al. Ketamine rapidly reverses stress-induced impairments in GABAergic transmission in the prefrontal cortex in male rodents. *Neurobiol Dis*. in press.
49. Ng LHL, et al. Ketamine and selective activation of parvalbumin interneurons inhibit stress-induced dendritic spine elimination. *Transl Psychiatry*. 2018;8(1):272.
50. Taylor SR, et al. GABAergic and glutamatergic efferents of the mouse ventral tegmental area. *J Comp Neurol*. 2014;522(14):3308--34.
51. Casanova E, et al. A CamKIIalpha iCre BAC allows brain-specific gene inactivation. *Genesis*. 2001;31(1):37--42.
52. Brigman JL, et al. Loss of GluN2B-containing NMDA receptors in CA1 hippocampus and cortex impairs long-term depression, reduces dendritic spine density, and disrupts learning. *J Neurosci*. 2010;30(13):4590--600.
53. Zhou F-W, et al. Balance of inhibitory and excitatory synaptic activity is altered in fast-spiking interneurons in experimental cortical dysplasia. *J Neurophysiol*. 2009;102(4):2514--25.
54. Potapenko ES, et al. Inhibitory-excitatory synaptic balance is shifted toward increased excitation in magnocellular neurosecretory cells of heart failure rats. *J Neurophysiol*. 2011;106(3):1545--57.
55. Budzillo A, et al. Dopaminergic modulation of basal ganglia output through coupled excitation--inhibition. *Proc Natl Acad Sci U S A*. 2017;114(22):5713--8.
56. Reynolds A, et al. Rational siRNA design for RNA interference. *Nat Biotechnol*. 2004;22(3):326--30.
57. Ventura A, et al. Cre-lox-regulated conditional RNA interference from transgenes. *Proc Natl Acad Sci U S A*. 2004;101(28):10380--5.
58. Koonsman J-P. The mouse brain in stereotaxic coordinates. *Psychoneuroendocrinology*. 2003;28(6):827--8.
59. Elsayed M, et al. Antidepressant effects of fibroblast growth factor-2 in behavioral and cellular models of depression. *Biol Psychiatry*. 2012;72(4):258--65.
60. Macbeth AH, et al. Housing conditions and stimulus females: a robust social discrimination task for studying male rodent social recognition. *Nat Protoc*. 2009;4(11):1574--81.

Figure Legends

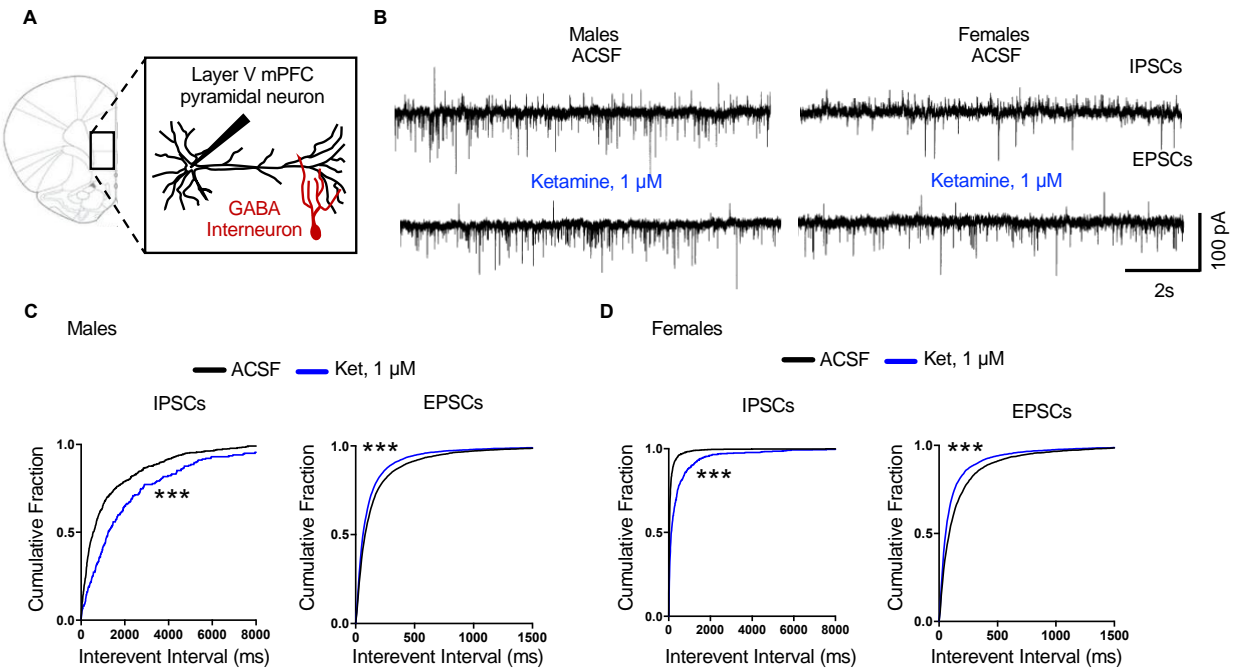


Figure 1. 1 μM ketamine reduces spontaneous inhibitory postsynaptic currents in mPFC slices. (A) Brain slice electrophysiology schematic. (B) Representative traces of spontaneous inhibitory postsynaptic currents (sIPSCs) and spontaneous excitatory postsynaptic currents (sEPSCs) from male and female mice before and after application of 1 μM ketamine (ket). (C) In male mice, 1 μM ketamine significantly decreases sIPSCs and increases sEPSCs (n=9-10 cells, 10 mice, ***, $P < 0.001$). (D) In female mice, 1 μM ketamine significantly decreases sIPSCs and increases sEPSCs (n=7-8 cells, 5 mice, ***, $P < 0.001$). Kolmogorov–Smirnov two-sample test was used. Data represented as the cumulative probability of the interevent interval. Abbreviations: ACSF = artificial cerebrospinal fluid, Ket = ketamine. Abbreviations: ACSF = artificial cerebrospinal fluid.

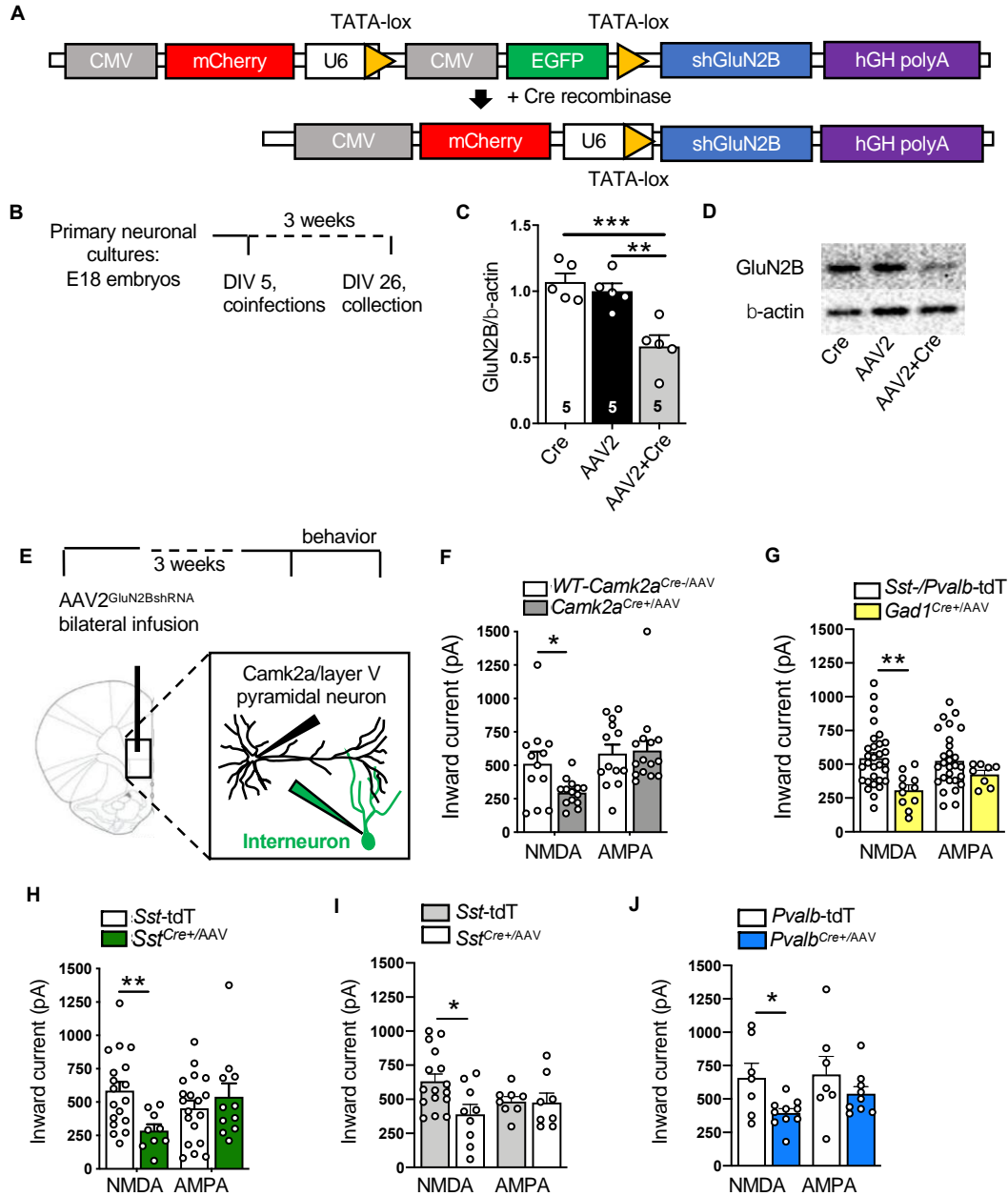


Figure 2. AAV2^{GluN2BshRNA} knocks down GluN2B and reduces NMDA inward currents in a Cre-dependent manner. (A) Schematic of the pGluN2BshRNA knockdown construct before and after introduction of Cre-recombinase to generate the active construct. (B) Schedule for cell culture experiments. (C) There was a significant reduction in GluN2B protein in the AAV2^{GluN2BshRNA}+AAV1-Cre (AAV2-Cre) group compared to AAV2^{GluN2BshRNA} (AAV2) or AAV2-Cre alone (Cre) (n=5 per group, one-way ANOVA with Tukey's multiple comparisons test,

($F_{2,12} = 14.1$, $P < 0.001$)). (D) Representative images of Western blots. Lanes were run on the same gel and were contiguous. (E) Schematic of the schedule for brain slice electrophysiology experiments. (F-J) The influence of AAV2^{GluN2BshRNA} on NMDAR and AMPAR inward currents was tested across genotypes. There was a significant reduction in NMDA-induced inward currents in all genotypes compared to their controls. Unpaired two-tailed t tests were performed. (F) *Camk2a*^{Cre+/AAV} (*Camk2a*^{Cre+/AAV}: n=3 mice, 14-15 cells; WT-*Camk2a*^{Cre+/AAV}: n=2 mice, 12-13 cells; $t_{24}=2.510$, $P=0.019$), (G) *Gad1*^{Cre+/AAV} (*Gad1*^{Cre+/AAV}: n=5 mice, 8-11 cells; *Sst*-/*Pvalb*-TdT-Tomato (TdT): n=10 mice, 28-30 cells; $t_{39}=3.447$, $P=0.0014$), (H) *Sst*^{Cre+/AAV} AAV males (*Sst*^{Cre+/AAV}: n=2 mice, 9-11 cells; *Sst*-TdT: n=8 mice, 16-17 cells; $t_{25}=2.976$, $P=0.006$), (I) *Sst*^{Cre+/AAV} females (*Sst*^{Cre+/AAV}: n=3 mice, 8-9 cells; *Sst*-TdT: n=9 mice, 8-16 cells; $t_{23}=2.686$, $P=0.013$), (J) *Pvalb*^{Cre+/AAV} males (*Pvalb*^{Cre+/AAV}: n=3 mice, 9-10 cells; *Pvalb*-TdT: n=5 mice, 7 cells; $t_{15}=2.696$, $P=0.017$). There were no significant differences in AMPA-induced inward currents in any genotype. *, $P < 0.05$, **, $P < 0.01$. All data are represented as mean \pm SEM. Abbreviations: tdT = td-Tomato.

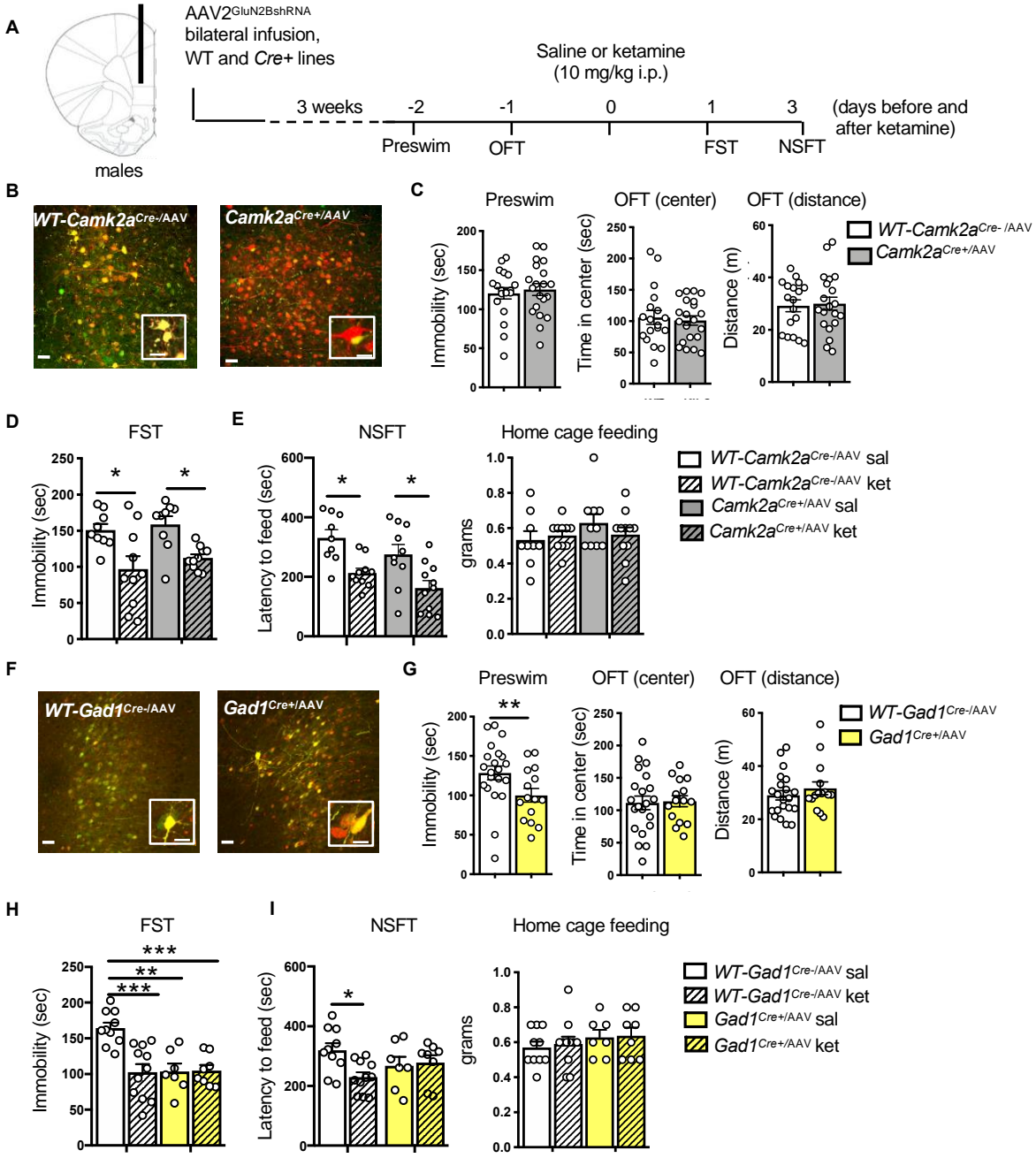


Figure 3. Infusion of AAV2^{GluN2BshRNA} into mPFC of *Gad1*^{Cre+}, but not *Camk2a*^{Cre+} male mice occludes the antidepressant effects of ketamine. (A) Procedure schematic. (B,F) Representative images of AAV2^{GluN2BshRNA} mediated expression and recombination in the mPFC of (B) wild-type (WT)-*Camk2a*^{Cre-}, *Camk2a*^{Cre+}, (F) *WT-Gad1*^{Cre-/AAV} and *Gad1*^{Cre+/AAV} male mice (scale bars = 50 μ m & 20 μ m in insets). (C) In *Camk2a*^{Cre+/AAV} mice, there was no effect of GluN2B knockdown

on baseline immobility (preswim) or time spent in center and distance traveled in the open field test (OFT; n=18-21 per group). (D) Both *WT-Camk2a^{Cre-/AAV-ket}* and *Camk2a^{Cre+/AAV-ket}* mice showed significantly reduced immobility in the forced swim test (FST) compared to saline controls (n=12-14 per group, treatment: $F_{1,34}=18.18$, $P=0.0002$). (E) Both *WT-Camk2a^{Cre-/AAV-ket}* and *Camk2a^{Cre+/AAV-ket}* mice showed significantly reduced latency to feed in the novelty-suppressed feeding test (NSFT; n=9-11 per group, treatment: $F_{1,36}=19.89$, $P < 0.0001$, genotype: $F_{1,36}=4.186$, $P=0.0481$). No significant differences were found in home cage feeding. (G) There was a significant reduction in preswim immobility in *Gad1^{Cre+/AAV}* mice, but no effect on time spent in center and distance traveled in the OFT (n=15-21 per group, $t_{34}=2.226$, $P=0.0327$). (H) Only *WT-Gad1^{Cre-/AAV-ket}* mice showed significantly reduced immobility in FST compared to their saline controls (n=7-11 per group, genotype: $F_{1,32}=8.662$, $P=0.006$, treatment: $F_{1,32}=9.313$, $P=0.0045$ genotype x treatment: $F_{1,32}=10.04$, $P=0.0034$). (I) Only *WT-Gad1^{Cre-/AAV-ket}* mice showed significantly reduced latency to feed in the NSFT (n=7-11 per group, genotype x treatment: $F_{1,32}=4.716$, $P=0.0374$). Preswim and OFT: unpaired two-tailed t-test. FST and NSFT: two-way ANOVA with Tukey's multiple comparisons. *, $P < 0.05$, **, $P < 0.01$, ***, $P < 0.001$. All data are represented as mean \pm SEM. Abbreviations: sal = saline, ket = ketamine.

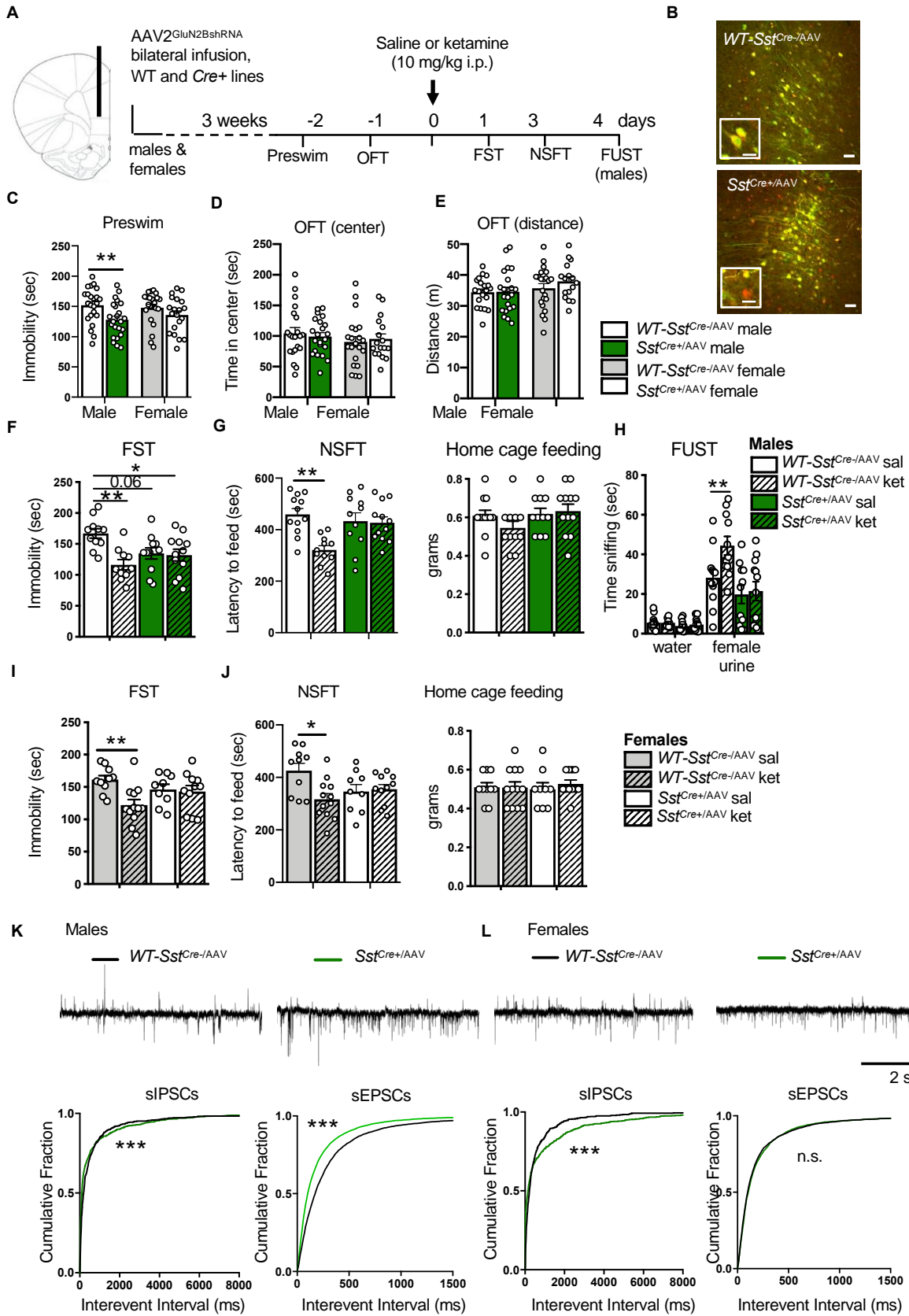


Figure 4. AAV2^{GluN2BshRNA} into mPFC of *Sst^{Cre+}* mice produces sex differences in baseline behavior and blocks the antidepressant effects of ketamine. (A) Procedure schematic. (B) Representative images of viral expression (scale bars=50 μ m & 20 μ m in insets). (C) GluN2B knockdown in *Sst^{Cre+}/AAV* mice reduced baseline immobility (preswim) in males compared to sex-matched controls (n=23 males, 20-22 females/group, males: $t_{44}=2.806$, $P=0.0075$) but did not affect time spent in center or distance traveled in the OFT (D,E; n=21-22 males, 17-22 females/group). (F,I) Only *WT-Sst^{Cre-}/AAV-ket* mice showed reduced immobility in the FST compared to controls (n=10-12 (f) and 9-12 (I) per group, males: treatment: $F_{1,40}=9.248$, $P=0.0041$, genotype x treatment: $F_{1,40}=7.453$, $P=0.0094$, females: treatment: $F_{1,38}=6.567$, $P=0.0145$, genotype x treatment: $F_{1,38}=4.744$, $P=0.0357$). (G,J) Only *WT-Sst^{Cre-}/AAV-ket* mice showed reduced latency to feed in the NSFT (n=11-12 (G) and 9-12 (J) per group, males: treatment: $F_{1,42}=9.171$, $P=0.0042$, genotype x treatment: $F_{1,42}=7.716$, $P=0.0081$, females: treatment: $F_{1,38}=4.454$, $P=0.0415$, genotype x treatment: $F_{1,38}=6.176$, $P=0.0175$). (G,J) No differences were observed in home cage feeding. (H) Only male *WT-Sst^{Cre-}/AAV-ket* mice showed increased time sniffing female urine in the FUST compared to controls (n=11-12 per group, genotype: $F_{1,84}=102.6$, $P<0.0001$, treatment: $F_{3,84}=6.199$, $P=0.0007$, genotype x treatment: $F_{3,84}=5.065$, $P=0.0028$) with no differences in time sniffing water. (K,L) Representative traces of sIPSCs or sEPSCs in layer V pyramidal neurons. (K) *Sst^{Cre+}/AAV* males had decreased sIPSCs and increased sEPSCs compared to controls (n=25-36 cells, 8-9 mice) (l) *Sst^{Cre+}* females had decreased sIPSCs but no differences on sEPSCs compared to controls (n=12-19 cells, 5 mice). Behavioral data: represented as mean \pm SEM. Preswim, OFT: unpaired two-tailed t-test. FST, NSFT: two-way ANOVA with Tukey's multiple comparisons. FUST: two-way ANOVA with Sidak's multiple comparisons. Electrophysiology data: represented as cumulative probability of the interevent interval (IEI). IEIs: Kolmogorov-

Smirnov two-sample test. *, $P < 0.05$, **, $P < 0.01$, ***, $P < 0.001$. Abbreviations: n.s.=non-significant.

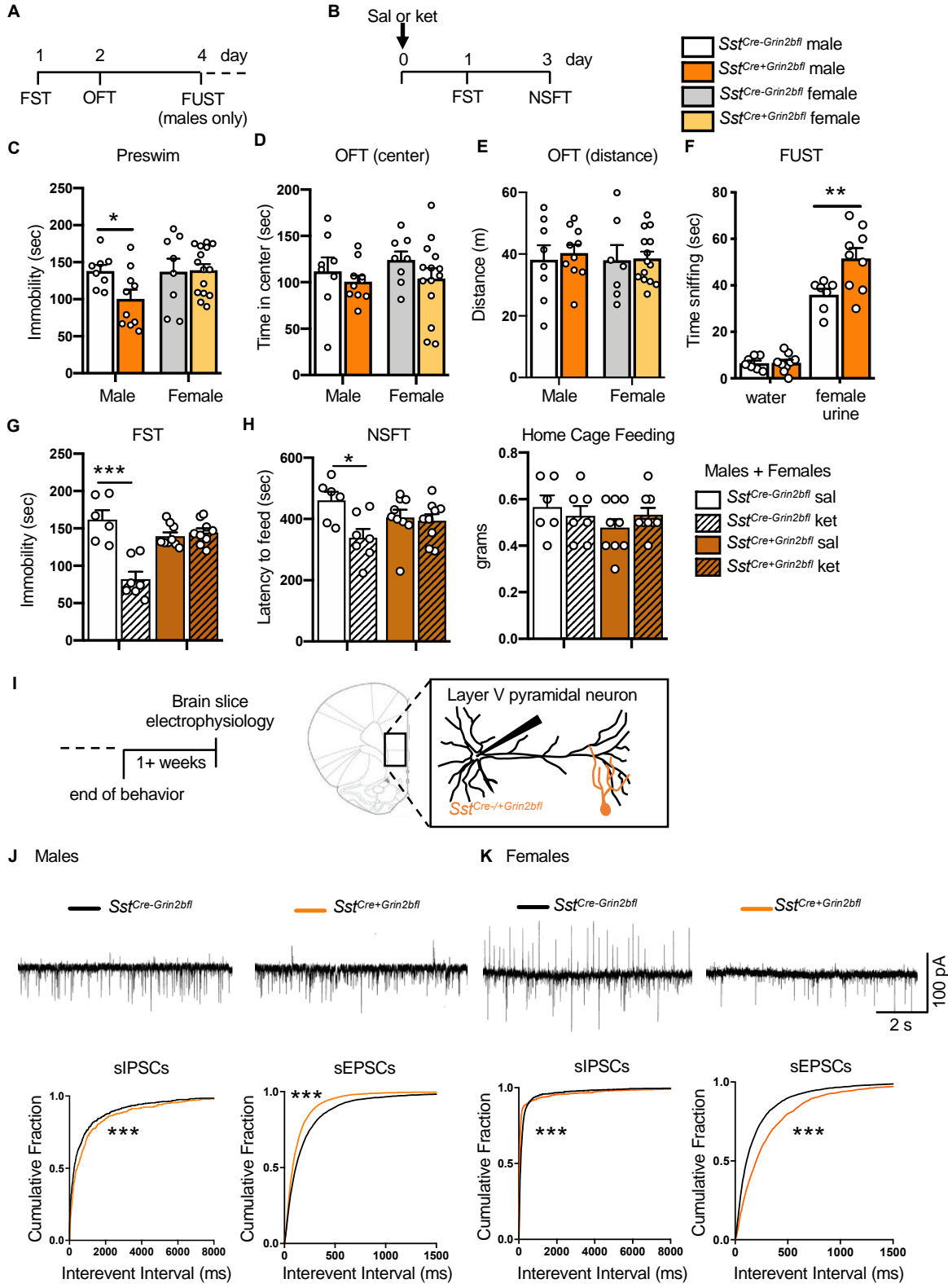


Figure 5. Genetic deletion of *Grin2b* from *Sst+* interneurons: behavioral and electrophysiological responses. (A,B) Procedure schematics for baseline (A) and post-ketamine (B) behaviors. (C) Only *SstCre+Grin2bfl* male mice have reduced baseline immobility (preswim) when compared to sex-match controls (*SstCre-Grin2bfl*; n=8-10 (males), 8-15 (females)/ group, males: $t_{16}=2.421$, $P=0.0277$). (D,E) There we no effects in *SstCre+Grin2bfl* mice on baseline time spent in center or distance traveled in the OFT compared to sex-matched controls (n=8-10 (males), 8-15 (females)/ group). (F) Male *SstCre+Grin2bfl* mice showed significantly more time sniffing female urine compared to controls in the FUST (n=7-9/ group, test: $F_{1,28}=163.3$, $P<0.0001$, genotype: $F_{1,28}=7.244$, $P=0.0119$, test x genotype: $F_{1,28}=7.069$, $P=0.0128$). (G,H) In a naïve group of male and female mice, only control *SstCre-Grin2bfl*-ket mice showed a significant reduction in (G) time spent immobile (n=6-9/ group, genotype: $F_{1,27}=6.67$, $P=0.02$, treatment: $F_{1,27}=23.1$, $P<0.0001$, genotype x treatment: $F_{1,27}=29.5$, $P<0.0001$) and in (H) latency to feed in the novelty-suppressed feeding test (NSFT), when compared to controls (n=6-9/ group, treatment: $F_{1,27}=6.54$, $P=0.02$, treatment x genotype: $F_{1,27}=4.56$, $P=0.04$). No significant differences were observed in home cage feeding. (I) Brain slice electrophysiology schematic. (J) Representative traces of sIPSCs and sEPSCs (K) Male *SstCre+Grin2bfl* mice had significantly decreased sIPSCs and increased sEPSCs compared to controls (n=20-23 cells, 7-9 mice). (L) Female *SstCre+Grin2bfl* mice had both significantly decreased sIPSCs and sEPSCs compared to controls (n=17-22 cells, 6-8 mice). Behavioral data are represented as mean \pm SEM. Preswim and OFT: unpaired two-tailed t test. FUST: two-way ANOVA with Sidak's multiple comparisons. FST and NSFT: two-way ANOVA with Tukey's multiple comparisons. Electrophysiology data are represented as the cumulative probability of the interevent interval (IEI). IEIs: Kolmogorov–Smirnov two-sample test. *, $P<0.05$, **, $P<0.01$, ***, $P<0.001$.

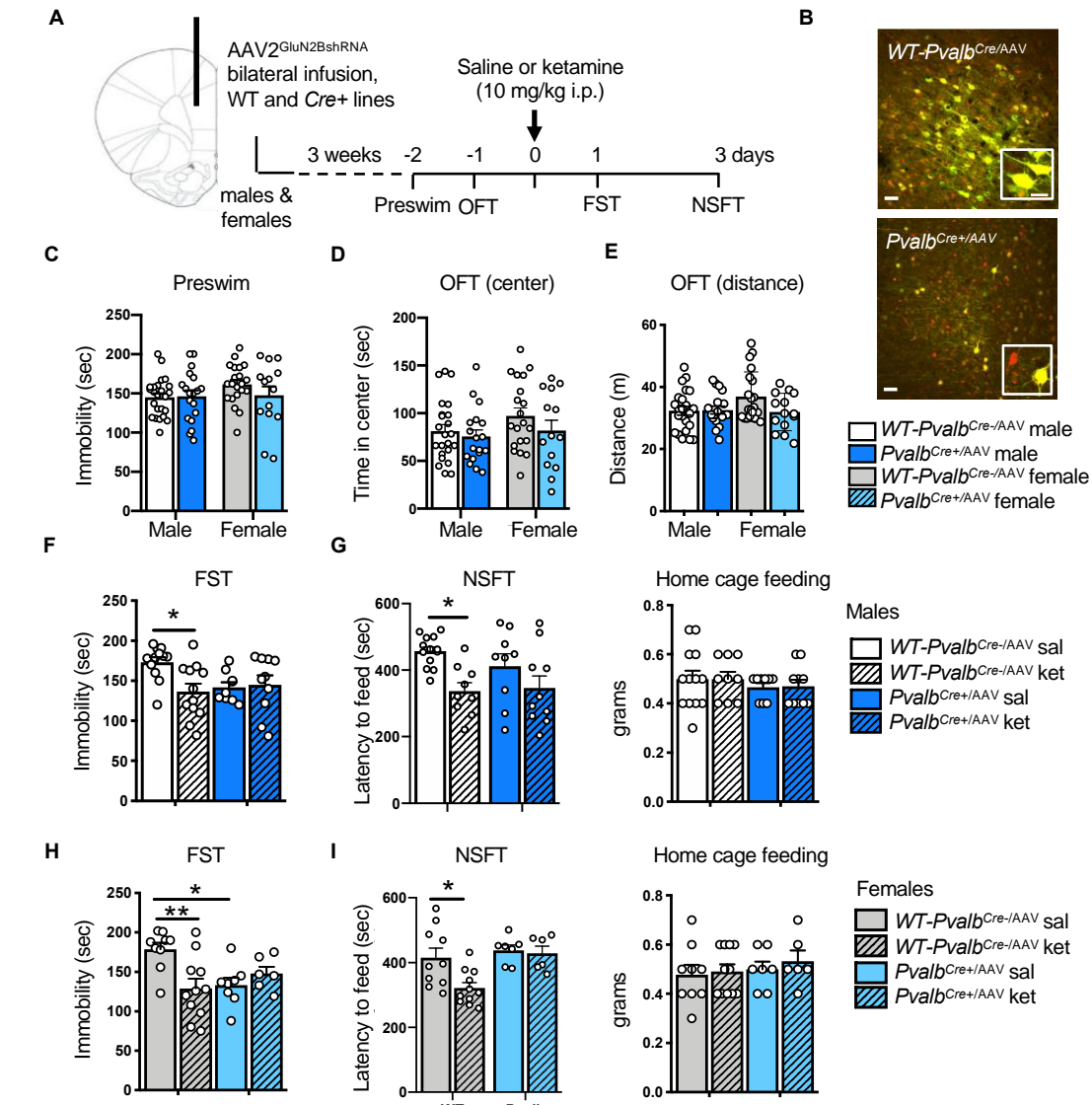


Figure 6. Infusion of AAV2^{GluN2BshRNA} into mPFC of *Pvalb*^{Cre+} male and female mice blocks the antidepressant effects of ketamine. (A) Procedure schematic. (B) Representative images of viral-mediated expression and recombination in the mPFC of WT-*Pvalb*^{Cre-/AAV} and *Pvalb*^{Cre+/AAV} mice (scale bars = 50 μ m & 20 μ m in insets). (C) GluN2B knockdown in *Pvalb*^{Cre+/AAV} mice had no effect on baseline immobility (preswim; n=19-24 (males) and 14-21 (females) per group). (D,E) GluN2B knockdown in *Pvalb*^{Cre+/AAV} mice had no effect on baseline time spent in center or distance traveled in the open field test (OFT), however there was a strong trend towards reduced

distance traveled in *Pvalb^{Cre+/AAV}* females (n=18-23 (males) and 14-20 (females) per group). (F,H) Only *WT-Pvalb^{Cre-/AAV}-ket* mice showed significantly reduced immobility in the forced swim test (FST) compared to their saline controls for both male (F) and female (H) mice; however, *Pvalb^{Cre+/AAV}-sal* female mice showed a significant reduction in immobility compared to *WT-Pvalb^{Cre-/AAV}-sal* females (n=9-12 (F) and 8-11 (H) per group, males: genotype x treatment: $F_{1,39}=5.1$, $P=0.0291$, females: genotype x treatment: $F_{1,30}=9.094$, $P=0.0052$). (G,I) Only *WT-Pvalb^{Cre-/AAV}-ket* mice showed significantly reduced latency to feed in the novelty-suppressed feeding test (NSFT) compared to controls for both (G) males and (I) females (n=9-13 (G) and 6-11 (I) per group, males: treatment: $F_{1,37}=10.91$, $P=0.0021$, females: genotype: $F_{1,30}=7.782$, $P=0.0091$, treatment: $F_{1,30}=4.926$, $P=0.0342$). All data are represented as mean \pm SEM. Preswim and OFT: unpaired two-tailed t tests performed within sex. FST and NSFT: two-way ANOVA with Tukey's multiple comparisons test. *, $P<0.05$, **, $P<0.01$